J. Phys. B: At. Mol. Phys. **18** (1985) 2021-2036. Printed in Great Britain

Total cross sections for electron scattering from Ar, Kr and Xe

R W Wagenaar and F J de Heer

FOM Institute for Atomic and Molecular Physics, Kruislaan 407, 1098 SJ Amsterdam, The Netherlands

Received 4 October 1984, in final form 11 December 1984

Abstract. Total cross sections have been remeasured for 20-100 eV electron scattering from Ar, Kr and Xe, achieving an accuracy of better than 5%. In the present measurements a short collision cell of adjustable length has been used, which permitted the application of higher target pressures than previously. Consequently, a more accurate determination of this parameter was possible, resulting in more reliable data for the total cross section. It appeared that below 70 eV the present data were substantially lower (at most 10%) than our previous ones and in very good agreement with the most recent experimental data of Nickel *et al.*

Because of the influence of effusion through the cell apertures, an experimental test had to be carried out on the effective gas density as a function of the cell length. This was also of critical importance for putting our differential cross section measurements on an absolute scale, as will be discussed in a subsequent article.

1. Introduction

A large number of experiments on total cross section measurements have previously been carried out as summarised in the review article of Bederson and Kieffer (1971). Generally, such an experiment consists of measuring the attenuation of the primary electron beam after passage through a collision chamber of a well defined effective absorption length. Most of the previous experiments have been performed using the Ramsauer (1921) technique, where the electron beam is energy selected with the aid of a magnetic field perpendicular to the orbital plane. Although Ramsauer's design is basically simple and elegant, it is difficult to control the spatial extension of the electron beam in such an arrangement. An unknown fraction of the scattered electrons may thus be registered in the detector; in particular at high impact energies this 'scattering in' effect can cause a considerable reduction in the measured absorption. Only a few decades later Golden and Bandel (1965) and recently Dalba *et al* (1979) could largely remove this serious shortcoming.

In their review Bederson and Kieffer (1971) reached the conclusion that, for instance in the case of helium, the existing data had an accuracy of at most 25% in the energy range up to 30 eV, whereas at higher energies the consistency was even worse. Therefore we (Blaauw 1979, Blaauw *et al* 1980) designed some apparatus, with which these data could be measured absolutely in the energy range 20-750 eV. A linearisation of the Ramsauer technique was used, avoiding the application of magnetic fields, and with an angular opening for detection of the attenuated beam which was sufficiently small

0022-3700/85/102021+16$02.25

to diminish the 'scattering in' effect mentioned before. The results of these measurements, together with a description of the apparatus, have been published in three separate articles: Blaauw *et al* (1980) for He and N_2, Wagenaar and de Heer (1980) for Ne, Ar, Kr and Xe and van Wingerden *et al* (1980) for H_2.

At about the same time as we initiated the present study, other groups also started experiments to obtain accurate data. They needed these as calibration standards for other measurements: for energy transfer calculations in the upper atmosphere or plasmas, or to compare with positron-atom collision studies. Apart from Dalba *et al* (1979), all these groups applied, just as we did, quite different techniques compared with Ramsauer's early design. At low energies (up to 12 eV) Milloy and Crompton (1977) carried out a diffusion experiment with a swarm technique, yielding momentum transfer cross sections which could then be transformed into total cross sections with high accuracy. For the low and intermediate energy range Kennerly and Bonham (1978) developed a nice technique. They recorded a time of flight spectrum with a pulsed electron beam, from which total cross sections could be derived simultaneously for all impact energies below 50 eV. Kauppila and coworkers (Kauppila *et al* 1977, 1981, Dababneh *et al* 1980, 1982, Hoffman *et al* 1982) performed both accurate total cross section measurements for electrons as well as for positrons over the broad energy range of a few eV up to about 500 eV in order to reveal typical energy-dependent differences between these two projectiles. Their device employs a longitudinal magnetic field for impact energy selection in combination with a retarding field element in front of the particle detector.

For He, Ne and N_2 our group found—in the overlapping energy ranges—agreement with these recent data within the combined error bars of typically 5–10%. As a result, a much more satisfactory situation does exist now. The data confirmed the excellency of the various recently refined theoretical calculations of total cross sections below the inelastic threshold for helium and neon. Of these recent calculations we mention the matrix variational method of Nesbet (1979) and the *R*-matrix calculations of Fon *et al* (1981). However, the various theoretical results at high impact energies (i.e. greater than about 100 eV), e.g. the distorted-wave second Born approximation (DWSBA) of Dewangen and Walters (1977) and the optical model of Byron and Joachain (1977) and McCarthy *et al* (1977), are less accurate; they converge only slowly to the experimental data with increasing impact energy.

For Ar, Kr and Xe our group (see Wagenaar and de Heer 1980) found some deviations from the results of Kauppila's group (Kauppila *et al* 1981, Dababneh *et al* 1982). This discrepancy could be ascribed for the main part to the imperfect screening against small-angle scattering in their set-up. After correction for this, a significant disagreement with them remained at impact energies below about 70 eV. Therefore we had to look for a possible systematic error in our measurements. The only possibility could be the uncertainty in the calibration of the pressure sensing head, which becomes critical at low target pressures (less than about 0.15 Pa). Since the scattering cross sections for the heavier noble gases are much larger than for helium and neon, in particular at the lower impact energies, and a large absorption has to be avoided, only small target pressures could be admitted in the 42 mm long collision cell which we used for the previous measurements.

We decided to remeasure these cross sections replacing the collision cell of 42 mm length in our apparatus by a new one of adjustable length (0.2–10 mm). Its short length enabled us to apply larger pressures, typically of the order of 1 Pa, and thus made the baratron reading less sensitive to possible zero shifts or calibration errors.

The earlier data for He and Ne were reproduced within the combined error bars, typically 2-4%. On the other hand, below about 60 eV the data for Ar, Kr and Xe deviated by 3-7% from our previous results and must now be considered as superceding these.

Before actually measuring these data, the effective product of target gas density and collision length had to be known exactly, because, since the collision cell is shortened, the density and profile of the gas will be influenced more and more by the effusive flow of the atoms and molecules through the entrance and exit orifices in the cell. These apertures are needed in order to let the primary and scattered beam pass. So far, this topic has led to some controversies in the literature. Several authors (Mathur and Colgate 1972, Mather *et al* 1975, Toburen *et al* 1968) derived different values for this parameter. Therefore a direct calibration was necessary. This we carried out with the help of a new analyser, equipped with a simultaneous particle detection technique (Wagenaar 1984). An extensive discussion of these results in comparison with the values we found from a computer simulation will be dealt with in the appendix of the present paper.

2. Experimental set-up and measurement procedure

2.1. General

The experiment is basically a linearisation of the Ramsauer technique; however, unlike the Ramsauer technique, there is no magnetic field present. This modification enables one to fix the scattering geometry unambiguously, so the angular resolution can be defined exactly.

The details of the apparatus have been described extensively by Blaauw *et al* (1980) and Wagenaar and de Heer (1980). As discussed before in the present set-up the former 42 mm collision cell has been replaced by one of adjustable length (0.2-10 mm). Instead of a retarding-field analyser for detection of the attenuated beam we used a rectangular shaped Faraday cage. We shall comment on the influence of these modifications.

2.2. Scattering geometry

The scattering geometry is defined by the aperture of the rectangular shaped Faraday cage (1 mm × 3 mm), which has been placed at a distance of 70 mm from the back plate of the collision cell, thus spanning a solid angle of 6.12×10^{-4} sr.

The evaluation of the total cross section σ_{tot} is based on the Lambert-Beer law:

$$\sigma_{\text{tot}} = (NL)^{-1} \ln(I_0/I_c) \tag{1}$$

where N stands for the gas density in the cell, L is the effective length of the electron path through the gas and I_0/I_c is the ratio of the beam intensity in front of and behind the absorption cell respectively. However, equation (1) represents the ideal case, in which the beam is infinitesimally narrow and the solid angle of the detector is zero. Of course, this situation is not feasible in practice and small-angle scattering must be incorporated. In the same way that equation (1) is derived, one finds:

$$\ln(I_0/I_c) = NL\sigma_{\text{tot}} - N \int_0^L \mathrm{d}x \int_0^{\Delta\Omega(x)} \frac{\mathrm{d}\sigma}{\mathrm{d}\Omega} \mathrm{d}\Omega. \tag{2}$$

Here, $\Delta\Omega(x)$ is the solid angle of the detector as seen in a scattering event taking place at position x on the beam axis. The factor $(d\sigma/d\Omega)$ represents (depending on the kind of detector) the elastic or elastic plus inelastic differential cross sections. It is essential to create experimental conditions under which the second term on the right-hand side of equation (2) is kept small with respect to the first term.

Previously, we used for intermediate and high electron energies (i.e. greater than about 35 eV) the retarding-field analyser with a solid angle of 7.8×10^{-5} sr and at low energies a Faraday cage with a relatively large solid angle of 3×10^{-3} sr. This switch in detection was necessary, because under vacuum conditions we are not able to tune the primary beam completely into the 1 mm diameter entrance aperture of the analyser at these lower energies. It was shown (Wagenaar and de Heer 1980) that, when measuring the attenuated beam intensity with the analyser as well as with the large Faraday cage, both modes yielded the same results within the statistical errors of 1% for all the noble gases under study for impact energies below 35 eV. Apparently, the contribution of the small-angle (in)elastic scattering to the total scattering yield is negligible at those energies. In the present set-up the opening angle of the new Faraday cage (6×10^{-4} sr) was about six times smaller than the one used before. Therefore, we could safely use this Faraday cage up to energies of about 100 eV, thereby neglecting the correction term of equation (2).

2.3. Adjustable collision-cell

We constructed a cell, whose length could be adjusted from 0.2–10 mm by means of a rack-and-pinion system, as shown in figure 1. The main purpose of making its length variable was to have an experimental check of the target gas density profile as a function of the collision length.

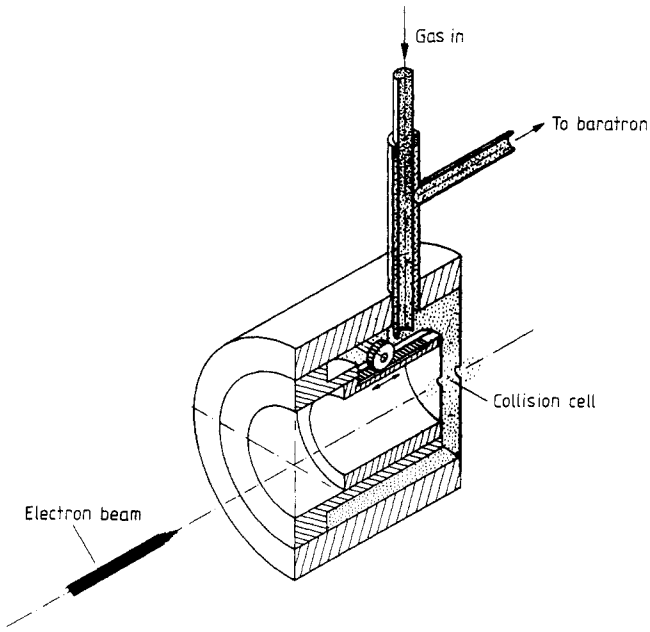

Figure 1. Construction details of the adjustable collision cell.

The cell is formed by the space between two molybdenum plates. The entrance plate has a diameter of 30 mm (and aperture diameter 1 mm) and the exit plate has a diameter of 68 mm (and aperture diameter 2 mm). Both apertures have been drilled in a conical shape towards the inner surface of the plates to avoid scattering of electrons and to approximate infinitesimally thin cell boundaries; otherwise, the apertures will establish short tubes of limited conductivity. The gas inlet consists of a narrow (internal diameter 3 mm) tube, which has been telescoped into an outer tube of internal diameter 8 mm. The gas flows into an annular space around the collision cell; through the outer tube it reaches the baratron sensing head. Apart from the thermal transpiration factor (see next section) no pressure drop will exist between the baratron and this annular space.

It should be mentioned here that the short collision cell is actually one of the modifications which we carried out before accurate small-angle differential scattering cross sections could be measured with this apparatus. The other major new element is a parallel-plate analyser with a channel-plate particle detection system. The rectangular shaped Faraday cage could be moved up and down pneumatically in front of the analyser's entrance slit. A detailed description of this analyser is given by Wagenaar (1984). Its only relevance in the present context is that it enabled us to check for a complete collection of the primary electron beam in the cup.

2.4. Experimental procedure and error discussion

2.4.1. Experimental procedure. The experimental procedure is based on the relation between the current attenuation and the total cross section as given by equation (1). Firstly, the electron optics are optimally adjusted, secondly, the current I_c in the Faraday cage behind the cell is measured and thirdly, the cup in front of the cell is moved downwards to intercept and measure the primary beam I_0. These currents are fed into a Keithly 610 electrometer; the meter delivers an output voltage proportional to the input current, which in its turn is fed into a microcomputer-controlled ADC to ensure accurate current readout. The total cross section is then derived by comparing the ratio (I_c/I_0) with and without gas in the collision chamber according to:

$$(I_c/I_0)_{gas}/(I_c/I_0)_{vac} = \exp(-NL\sigma_{tot}). \tag{3}$$

In order to obtain reliable data, it is further necessary to determine L and N very accurately.

Since the pressure is measured with a baratron, kept at an elevated temperature of 322 K, there exists a small pressure drop over the tube which connects the baratron with the gas cell. As previously reported by us (Blaauw *et al* 1980), this thermal transpiration does not necessarily obey the Knudsen (1910) law at low P:

$$D = (P_c/P_h) = (T_c/T_h)^{1/2} \tag{4}$$

where the indices c and h refer to the low and high temperature regions respectively. Instead, D appears to depend on the specific dimensions of the connecting elements and tubes between the pressure gauge and gas cell. Therefore, we performed the same test as before with two sensing heads, one at 322 K and the other at room temperature, symmetrically connected with the gas cell. The outcome of this test reconfirmed the results found with the fixed 42 mm long collision cell (see figure 4 of Blaauw *et al* 1980). As long as the pressures are kept below about 4 Pa, D retains a constant value of 0.98, whereas at higher pressures this drop disappears, i.e. D becomes unity.

Having established the correct relation between the local pressure in the baratron head and the collision cell region, we are left with the problem of determining the effective absorption length. At the typical pressures applied, the mean free path length of the target gas atoms is generally considerably larger than the dimensions of the cell. One thus deals with effusive molecular flow through the entrance and exit apertures, where the gas will possess large density gradients. As such, the product (NL) in the exponent of equation (3) has to be replaced by

$$(NL)_{\text{eff}} = \int_{\text{S}}^{\text{D}} n(z)\,\mathrm{d}z. \tag{5}$$

This definite integral, with limits from particle beam source (S) to detector (D), accounts for the non-uniform distribution $n(z)$ of scattering gas along the beam path. It is more convenient to define a correction factor α such that:

$$\int_{\text{S}}^{\text{D}} n(z)\,dz \equiv \alpha NL \tag{6}$$

where N is the density as measured with the baratron (corrected for thermal transpiration) and L the geometrical length of the collision cell. Several approaches for calculating α are available in the literature, but the results deviate strongly from each other (see Blaauw *et al* 1980). The quantity α is critically dependent on the adjustable length of the new collision chamber. When this cell is shortened, one enters a regime where, according to Mathur *et al* (1975), α decreases substantially. Therefore, we investigated the range of L, where α is still essentially equal to unity. In figure 2 the logarithm of the absorption ratio has been plotted as a function of the cell length, where Kr has been used as target gas. The points are the averages of the values found at various pressures; this clearly demonstrates a linear behaviour for L values larger

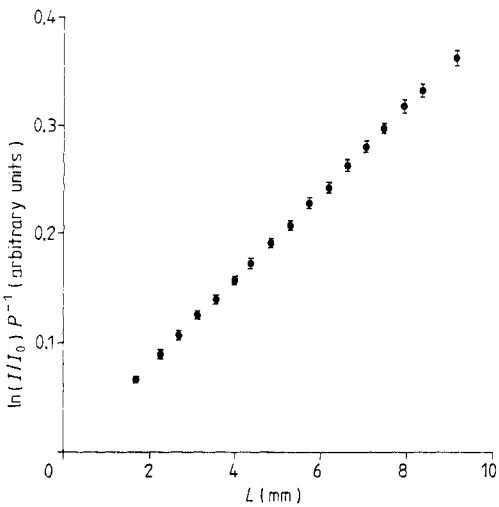

Figure 2. Logarithm of the absorption ratio divided by the pressure as a function of the cell length. The points are averages of the values found at various krypton pressures. For $L > 4$ mm all points lie on a straight line, which crosses the X axis at $L = 0$.

than about 4–5 mm, which means that α is approximately equal to 1.0. The present cross section measurements were performed with the cell adjusted to 4.5 mm.

In the appendix we discuss the results of a more sensitive test which we conducted to find the behaviour of α when L is reduced to almost zero. To that end we made use of the parallel-plate analyser to register the number of scattered electrons per unit time and beam current, since this number is directly proportional to the target gas density N.

Having established all the parameters involved, equation (3) finally leads to the next expression for σ_{tot}:

$$\sigma_{tot} = -0.5 \frac{(T_c T_m)^{1/2}}{P_m L} \ln[(I_c/I_0)_{gas}/(I_c/I_0)_{vac}] \tag{7}$$

where σ_{tot} is in a_0^2, T_c and T_m are the temperatures in K in the gas cell and baratron head respectively, P_m is the baratron pressure in Pa and L is the cell length in cm. The numerical value of 0.5 has been arrived at by taking the experimentally derived thermal transpiration ratio into account.

The independence of σ_{tot} on the gas pressure and beam current was established for each gas at three different impact energies.

The energy of the electron beam was calibrated by measuring the position on the energy scale of the pronounced 19.3 eV resonance for electron-helium scattering (Blaauw *et al* 1980). A possible contribution from aperture scattering was investigated by measuring σ_{tot} at various cell lengths where α is approximately equal to 1.0. Since no significant difference was found among the σ_t values obtained thus, such back scattering did not affect the final results.

2.4.2. Error discussion. The measurements are subject to the same error sources as mentioned by Blaauw *et al* (1980). In comparison with the former results, the accuracy in measuring the pressure has increased, whereas the exact determination of the absorption length becomes somewhat more critical. Table 1 summarises the experimental errors; the systematical errors are all maximum estimates, whereas the statistical error is given with an estimated standard deviation of only 1%.

Table 1. Survey of the experimental errors.

Error source	Error estimation (%)
Statistical	$\leqslant 1$
Systematical	
(*a*) interaction length	$\leqslant 1.5$
(*b*) baratron calibration	$\leqslant 0.5$
(*c*) linearity current meters	$\leqslant 0.5$
(*d*) energy definition,	
(i) for impact energies above about 50 eV	$\leqslant 0.5$
(ii) for impact energies below about 50 eV	$\leqslant 1.5$
Total error	
(i) below about 50 eV	$\leqslant 5$
(ii) above about 50 eV	$\leqslant 4$

3. Results and discussion

An extensive discussion of our previous experimental results on total scattering of electrons from Ar, Kr and Xe has been given by Wagenaar and De Heer (1980), where comparison has been made with other experiments and theory. These data covered the impact energy range 20-750 eV. A summary of the main conclusions of that paper has been presented in the introduction, where we noted that the discrepancy between the data of Kauppila *et al* (1981) and Dababneh *et al* (1982) and ours could not be explained completely at low and intermediate energies (below about 100 eV). With our new results, which are confirmed by the recent measurements of Nickel *et al* (1983) and Jost *et al* (1983), more clarity is provided in this problem.

First, looking at table 2 for argon, we now find agreement within 5% with Kauppila *et al* (1981). Their 5-10% lower values at high energies can be corrected when incomplete screening against electrons scattered over small angles is taken into account. The cut-off angle in their apparatus was on average 6°, whereas this amounted in our set-up to only 0.3-0.5°. With the optical model calculations of Joachain *et al* (1977) they estimated the contribution of the integral expression in equation (2) to be 9% at most. However, below 40 eV their values still remain too low when corrected for this effect.

Evidence for the accuracy of our data is given by the results of Nickel *et al* (1983) and Jost *et al* (1983), who both agree within 5% with us at all energies of overlap. The agreement with Nickel *et al* is the more convincing, since the basic features of their apparatus—of the same linear absorption type as our design—are a low cut-off angle (less than 1°) for small-angle elastic scattered electrons and a complete screening against inelastic scattering.

Table 3 shows the results for krypton. As said before, our previous data were substantially higher than those of Dababneh *et al* (1982): 15% at 20 eV to 7% at 100 eV. The remeasured data are in much better agreement with them; the relative difference has been reduced to a constant value of 3-5% for all energies below about 250 eV. However, this good agreement in relative shape is disrupted seriously if we apply Dababneh's estimated corrections (up to 15%) for small-angle scattering based on the optical model calculations of McCarthy *et al* (1977). Clearly, in practice their apparatus screens much better against these scattered electrons.

The cross sections of Jost *et al* (1983) show a stronger increase towards lower impact energies than ours; besides, their values are probably too low (about 10%) in the intermediate energy range. Given the excellent agreement with them for argon, it is not clear which experimental error is involved here. On the other hand, their method of deriving cross sections—measuring absorption ratios with a set of collision cell exit slits of different width and then linearly extrapolating the values thus obtained to zero width—can overestimate the 'scattering in' effect involved, since the differential cross section has a tendency to level off towards zero angle at these energies; too large cross sections at lower energy may thus be found.

The results for xenon are presented in table 4. Again, the data of Kauppila's group (Hoffman *et al* 1982) remain substantially lower than our remeasured values: from 5% at 20 eV to a constant difference of about 10% above 100 eV. Perfect agreement (<3%) is found with Nickel *et al* (1983), whereas the data of Jost *et al* (1983) possess a stronger increase towards lower energies, probably for the same reason as with krypton.

The semiempirical cross sections of de Heer *et al* (1979) clearly deviate from the results of all experimental groups below about 100 eV. Recently, Hayashi (1983) redetermined total excitation cross sections σ_{exc} for electron-xenon scattering by carrying out the following profound procedure. First, he selected recommended values of elastic momentum transfer and ionisation cross sections. Secondly, he applied a scaling law to Eggarter's (1975) σ_{exc} data for argon, which were about twice the values

Table 2. Total cross sections for electron-argon scattering in units of a_0^2.

	Experiment			
E (eV)	This work†	K	N	J
7.5			54.7	53.5
10.0			73.4	71.4
12.5			84.8	86.4
15	(82.76)	77.0	84.3	85.3
17.5	76.72 (79.42)		74.7	76.7
20	68.75 (73.70)	61.9	67.9	68.9
22.5	62.55 (67.02)			62.1
25	56.81 (60.52)		57.9	57.8
27.5	51.33 (54.94)			53.9
30	48.76 (50.72)	46.2	51.8	50.7
35	44.83 (46.41)			46.0
40	41.94 (53.40)		43.1	42.8
45	38.27 (39.92)			40.1
50	36.65 (37.30)	35.5	38.2	37.5
55	35.16 (35.53)			35.7
60	34.55		35.3	34.3
65	34.10			
70	33.23		33.3	
75	32.49	29.9		
80	31.80		31.4	
90	30.62		29.9	
100	29.60	27.4	28.5	
125	27.35		25.9	
150	25.13	22.7	23.7	
175	23.03			
200	21.33	20.0	20.8	
250	18.92		18.6	
300	17.47	16.4	17.1	
350	16.09			
400	14.91	13.7		
450	13.92			
500	13.08	11.7		
550	12.35			
600	11.71	10.5		
650	11.15			
700	10.62	9.52		
750	10.13			

† Values in parentheses have been superseded (Wagenaar and de Heer 1980).
K, Kauppila *et al* (1981).
N, Nickel *et al* (1983).
J, Jost *et al* (1983).

of de Heer *et al* in the energy range 20–50 eV; the resulting σ_{exc} data for xenon merged with de Heer's data first at 300 eV. From the thus constructed data he was able to derive values for the Townsend ionisation coefficient α, which are rather sensitive to the σ_{exc} chosen. Comparing these values for α with those obtained from swarm experiments showed agreement only if Eggarter's σ_{exc} data had been used as input,

Table 3. Total cross sections for electron-krypton scattering in units of a_0^2.

	Experiment		
E (eV)	This work†	D	J
7.5		82.4	88.2
10.0		95.3	100.3
12.5		97.1	98.9
15		91.9	92.8
17.5		86.8	86.0
20	84.67	81.1	80.3
22.5	79.93 (87.16)	75.6	75.3
25	74.48 (81.28)	71.8	71.5
27.5	70.82 (76.50)	68.47	67.2
30	68.45 (72.63)	66.70	62.1
35	63.77 (66.94)	61.36	59.6
40	59.42 (62.99)	58.85	56.0
45	56.86 (59.90)	53.96	52.8
50	54.23 (56.71)	53.03	50.1
55	52.65 (54.27)		47.8
60	51.35 (52.33)		46.0
65	50.56		
70	48.76		
75	46.85	42.27	
80	45.04		
85	43.39		
90	41.83		
95	40.38		
100	39.04	37.02	
125	33.92	33.41	
150	30.68	30.52	
175	28.88	27.66	
200	27.68	26.38	
250	25.32	23.34	
300	22.81	21.31	
350	20.80	19.77	
400	19.25	18.10	
450	18.12	16.96	
500	17.12	15.96	
550	16.26	14.96	
600	15.54	14.31	
650	14.90	13.49	
700	14.29	12.92	
750	13.67	12.56	

† Values in parentheses have been superseded (Wagenaar and de Heer 1980).
D, Dababneh *et al* (1980, 1982).
J, Jost *et al* (1983).

clearly demonstrating that the values for σ_{exc} at lower energy as estimated by de Heer were too low. Summing up all contributions to the total cross section now yields values well in accordance with the experimental data below 100 eV, as can be seen from table 4.

Table 4. Total cross sections for electron-xenon scattering in units of a_0^2.

	Experiment				Semi-empirical	
E (eV)	This work†	D	N	J	H	Ha
7.5		144.6	149.2	173.5		
10.0		138.1	143.3	158.1		139.2
12.5		132.8	137.9	147.1		
15		126.8	132.1	137.8		132.0
17.5		123.9	131.1	134.2		
20	126.7 (133.0)	119.6	127.7	131.0	110.2	124.9
22.5	114.9 (123.5)	110.9		122.1		
25	102.6 (110.1)	96.1	98.9	107.4		
27.5	87.60 (94.73)	81.5		92.8		
30	74.45 (79.85)	71.99	74.2	81.0		73.7
35	61.08 (64.95)	59.81		66.7		
40	55.95 (58.62)	53.45	56.1	58.9		
45	53.27 (55.64)	50.74		53.9		
50	50.83 (53.10)	46.81	49.8	50.7		48.4
55	49.16 (50.27)			49.3		
60	47.55 (48.25)		47.1	48.2	36.85	
65	46.90					
70	46.19		45.2			
75	45.92	41.59				
80	45.63		44.1			
85	45.15					
90	44.63		43.3			
95	44.07					
100	43.51	38.66	42.5		38.10	41.2
125	41.44	37.19	39.7			
150	39.40	34.91	37.9		35.51	
175	37.61	33.16				
200	36.02	32.48	35.4		34.24	34.9
250	33.27	30.02	32.8			
300	30.95	28.09	30.5		27.80	30.3
350	28.93	26.06				
400	27.32	24.70			25.56	
450	25.83	22.92				
500	24.53	21.92			22.36	24.3
550	23.40	20.70				
600	22.38	19.24				
650	21.45	18.38				
700	20.56	18.45			18.40	
750	19.68	17.38				

† Values in parentheses have been superseded (Wagenaar and de Heer 1980).
D, Dababneh *et al* (1980, 1982).
N, Nickel *et al* (1983).
J, Jost *et al* (1983).
Ha, Hayashi (1983).
H, de Heer *et al* (1979).

4. Conclusions

Total cross section measurements have been presented for electron scattering from Ar, Kr and Xe, claiming an accuracy of better than 5% and performed under very well defined conditions of angular resolution. Particular care had to be taken at the lower impact energies in the precise determination of the target gas pressure for krypton and xenon; with a shorter collision cell we could refine our previous measurements. Our apparatus yielded systematically higher values than most experiments performed before 1983; the explanation must be found in a more complete compensation for forward scattering in our set-up than achieved by others. Indeed, for argon good agreement is found with the data of Kauppila and coworkers if their suggested correction for this effect is taken into account. However, the near constant difference between their krypton and xenon data and ours cannot be corrected for by a better angular screening only. As such it points to some calibration error. The confidence in our xenon data has just recently been strengthened by the measurements of Trajmar and coworkers (Nickel *et al* 1983) and Jost *et al* (1983), who both chose the same scattering geometry as we did.

Appendix. Effective gas density in short scattering chambers

In this appendix we investigate the influence of apertures in short cylindrically shaped collision chambers on the gas density distribution n along the z axis. In § 2.3 a factor α was introduced, which accounts for the non-uniformity of $n(z)$ along the beam axis due to the effusive gas flow through the orifices (see equation (6)) and suggested that its value will become smaller than unity when the actual cell length is shortened.

It is our purpose here to compare the results for α obtained from a computer simulation with those we found experimentally. The latter were obtained by counting the number of scattered electrons in a fixed angular range as a function of L, thereby keeping a constant density N as measured by the baratron. This procedure was justified, since L was always at least an order of magnitude smaller than the distance between cell and channel-plate detector. The computer model is basically the same as proposed by Mathur *et al* (1975), but we extended it to our cell configuration with apertures of unequal diameter.

Consider the case of a rarefied gas, confined in a cylindrically shaped volume, where the gas phase collisions are practically negligible compared with molecular impacts on the walls, and where the walls reflect molecules diffusively according to the cosine law. The first condition is generally satisfied since the mean free path is usually long compared with chamber dimensions. Compliance with the second condition is more difficult to establish with general confidence, but at room temperature and below, the reflection mechanism may be considered to involve an intermediate step of temporary adsorption on the walls and subsequent evaporation whereby the memory of the incident direction is lost, giving a cosine distribution.

The contribution to the local number density near a point P in the body of a gas by molecules diffusively reflected from a surface element dS on a wall is:

$$dn_P = n_s(d\omega/4\pi)\cos\theta \tag{A.1}$$

where $d\omega$ is the solid angle subtended at P by the surface element in question and n_s is the effective equilibrium gas density at which the element appears to reflect, shown

in figure 3(a). The factor cos θ accounts for the diffusive reflection where the angle θ is defined with respect to the normal on the wall surface. The total number density at P is found by integrating the above equation over all of the walls and, if present, source regions exposed to P:

$$n_P = \frac{1}{4\pi} \int n_s \cos\theta \, d\omega. \tag{A.2}$$

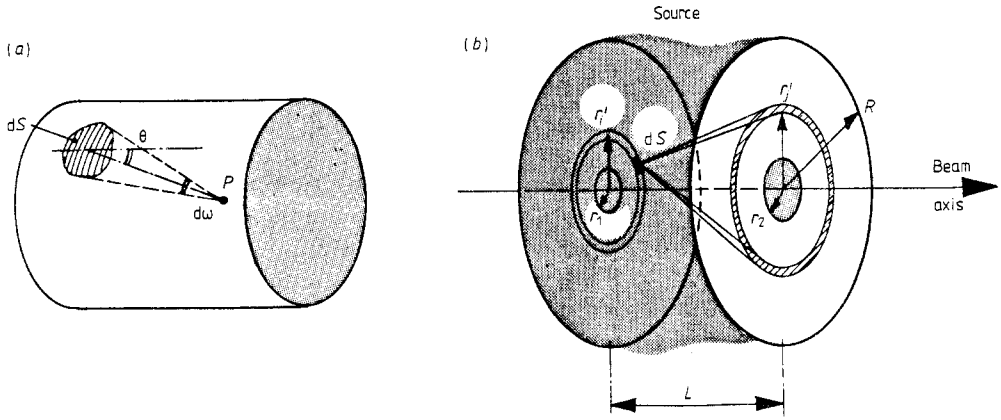

Figure 3. (a) Solid angle subtended at a point P inside the cell by a wall surface element dS. (b) Geometry and notation used to evaluate the incident flux on a flat ring of radius r_i' due to reflection from a flat ring of radius r_i' at the opposite cell wall. A steady flow of gas from the annular source region is assumed throughout the calculations.

The following parameters fix the cell geometry: L is the length of the cell, r_1 and r_2 the radii of the entrance and exit aperture respectively and R the cell wall radius. The walls are assumed to be of negligible thickness (i.e. the apertures are of knife-edge shape). Further, let the cylindrical walls be divided into circular rings of equal width, as in figure 3(b). The computational scheme then proceeds by calculating the incoming flux of particles onto each ring coming from the opposite cell plate and the source region. After a sufficient number of iterations, the equilibrium density at each ring can be obtained, where the rate of reflection from the surface elements equals the rate of molecular incidence on them. During the whole iteration process, the density N at the annular source boundary R is kept constant.

Figure 4 shows a typical density gradient along the walls for our cell geometry with $L = 2$ mm, obtained after 21 iterations with 60 rings. The densities in opposite rings become clearly different from eath other in the neighbourhood of the apertures, since these are unequal in size.

Having determined the effective densities at the walls, it is now a simple matter with the help of equation (A.2) to calculate the equilibrium density in each point inside and outside the cell. Solving equation (6) with Simpson's integration rule, using values of $n_i(z_i)$, finally yields the required parameter α. These are displayed in table 5 as a function of L at three ratios of r_1/r_2; in all cases we fixed $R/r_1 = 20$. Within parentheses we have added the values of Mathur *et al* (1975) calculated for $r_1/r_2 = 1.0$.

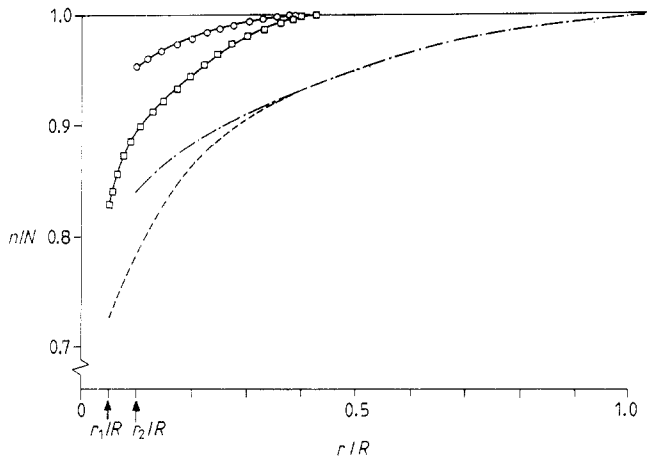

Figure 4. Density gradients along the circular cell walls due to effusing of the gas through the apertures, shown for two cell-plate radii (R and $R/2$). The displayed densities have been normalised on the source density N; the ratio $r_1/r_2 = 0.5$ (see text). - · -, exit plate, $n = N$ at $r = R$; - - -, entrance plate, $n = N$ at $r = R$; ○-○, exit plate, $n = N$ at $r = R/2$; □-□, entrance plate, $n = N$ at $r = R/2$.

The values in table 5 only depend on the ratio of aperture size over collision cell length, not on the absolute magnitude of these quantities. The values for α at $r_1/r_2 = 0.5$ are shown in figure 5 together with the experimental results, where r_1 was fixed at 0.5 mm and argon used as target gas. The experiment yields significantly higher α values than those derived from the computer model; already at $L = 2.5$ mm we found $(1.00 - \alpha_{exp}) < 0.01$. Noteworthy here is the fact that the experimental check Mathur performed on his calculated data also resulted in higher values than his model predicted. He attributed this deviation to the finite thickness of the cell plates; as such, the apertures would present extra channels with corresponding small conductivities. Whereas this might be the case for the cell he used, our results on the other hand exclude such a mechanical cause: as can be seen from figure 2, our data at $L > 2.5$ mm lie on a straight line, which, when extrapolated down to signal $S = 0$, definitely crosses the axis at $L = 0$.

In order to find the cause for the observed discrepancy, one has to examine the basic assumptions in the model more critically. We checked $\dot{\alpha}$ at various pressures

Table 5. Calculated values for α at various ratios of the cell length L over the entrance aperture radius r_1; three different exit aperture radii have been considered.

L/r_1	$\alpha\ (r_2 = r_1)$	$\alpha\ (r_2 = 2r_1)$	$\alpha\ (r_2 = 3r_1)$
0.5	0.45	0.29	0.24
1.0	0.58 (0.61)	0.44	0.38
1.5	0.69	0.56	0.49
2.0	0.79 (0.80)	0.66	0.58
3.0	0.88 (0.89)	0.76	0.70
4.0	0.93 (0.93)	0.86	0.80
6.0	0.97	0.93	0.88

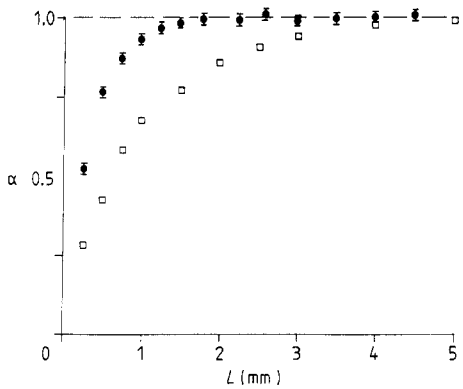

Figure 5. Calculated values for the correction factor α from the computer model (□) and numbers derived from experiment (●) where argon was used as a target gas. The entrance and exit aperture diameters were respectively 1.0 and 2.0 mm.

ranging from 0.1-3 Pa. No dependence for α on this parameter was found, so the assumption with respect to the mean free path length seems to be correct. As said before, the assumption of diffuse reflection is not directly amenable to experimental tests. An argument against a pure cosine distributed reflection mechanism can be put forward, when the steep density drop along the walls towards the apertures is considered more critically in figure 4. Since noble-gas atoms are only weakly bound at the wall surface during a collision, part of them will 'creep' over the surface before evaporating back into the vacuum. As such, a thin gas layer may be attached to the walls. The density gradient may then work as a pump on it and consequently a small diffusion current is set going to raise the gradient. The net result is that part of the incoming flux is pumped towards the apertures instead of being diffusively reflected. If this effect contributes significantly, one should expect it to be gas dependent. However, experimental tests carried out for helium, argon and krypton did not reveal an observable difference among these gases. Apparently, the free path length of these noble-gas atoms are too large compared with the installed cell lengths and their binding energies too small in order to observe gas-dependent effusion effects.

Another approach should consist of building other reflection distributions into the model. It is likely that part of the particles will not reflect diffusively, but instead specularly.

Two main conclusions can be drawn from the preceding analysis. First, the gas density drop is not as drastic as one would expect on the basis of simple gas dynamics with diffusive reflection from surrounding walls. Further research, with the emphasis on models other than diffusive reflection only, is necessary in order to provide widely applicable model calculations. The second conclusion is that the generally adopted standard of considering the effective absorption length as the actual cell length augmented with the sum of the aperture diameters lacks any justification. Only if thick cell walls or high pressures are used, will it indeed approach the real situation.

Acknowledgment

The authors wish to thank Dr W Koot for assistance in the measurements of the effective collision length and Dr S Trajmar and Dr K Jost for providing data before

publication. This work is part of the research program of the Stichting voor Fundamenteel Onderzoek der Materie (Foundation for Fundamental Research on Matter) and was made possible by financial support from the Nederlandse Organisatie voor Zuiver-Wetenschappelijk Onderzoek (Netherlands Organization for the Advancement of Pure Research).

References

Bederson B and Kieffer L J 1971 *Rev. Mod. Phys.* **43** 601
Blaauw H J 1979 *PhD Thesis* University of Amsterdam
Blaauw H J, Wagenaar R W, Barends D H and de Heer F J 1980 *J. Phys. B: At. Mol. Phys.* **13** 359
Byron F W and Joachain C J 1977 *Phys. Rev.* A **15** 128
Dababneh M S, Hsieh Y F, Kauppila W E, Pol V and Stein T S 1982 *Phys. Rev.* A **26** 1252
Dababneh M S, Kauppila W E, Downing J P, Laparrière F, Pol V, Smart J H and Stein T S 1980 *Phys. Rev.* A **22** 1872
Dalba G, Fornasini P, Lazizzera I, Ranieri G and Zecca A 1979 *J. Phys. B: At. Mol. Phys.* **12** 3787
Dewangen D P and Walters H R J 1977 *J. Phys. B: At. Mol. Phys.* **10** 637
Eggarter E 1975 *J. Chem. Phys.* **62** 833
Fon W C, Berrington K A and Hibbert A 1981 *J. Phys. B: At. Mol. Phys.* **14** 307
Golden D E and Bandel H W 1965 *Phys. Rev.* **138** A14
Hayashi M 1983 *J. Phys. D: Appl. Phys.* **16** 581
de Heer F J, Jansen R H J and van der Kaay W E 1979 *J. Phys. B: At. Mol. Phys.* **12** 979
Hoffman K R, Dababneh M S, Hsieh Y F, Kauppila W E, Pol V, Smart J H and Stein T S 1982 *Phys. Rev.* A **25** 1393
Joachain C J, Vanderpoorten R, Winters K H and Byron F W 1977 *J. Phys. B: At. Mol. Phys.* **10** 227
Jost K, Bisling P G F, Eschen F, Felsmann M and Walther L 1983 *Proc. 13th Int. Conf. on Physics of Electronic and Atomic Collisions, Berlin* ed J Eichler *et al* (Amsterdam: North-Holland) p 91 and private communication
Kauppila W E, Stein T S, Jesion G, Dababneh M S and Pol V 1977 *Rev. Sci. Instrum.* **48** 822
Kauppila W E, Stein T S, Smart J H, Dababneh M S, Ho Y K, Downing J P and Pol V 1981 *Phys. Rev.* A **24** 725
Kennerly R E and Bonham R A 1978 *Phys. Rev.* A **17** 1844
Knudsen M 1910 *Ann. Phys., Lpz* **31** 205
Mathur M P and Colgate S O 1972 *Phys. Rev.* A **6** 1266
Mathur M P, Field J E and Colgate S O 1975 *Phys. Rev.* A **11** 830
McCarthy I E, Noble C J, Phillips B A and Turnbull A D 1977 A **15** 2173
Milloy H B and Compton R W 1977 *Phys. Rev.* A **15** 1847
Nesbet R K 1979 *Phys. Rev.* A **20** 58
Nickel J, Imre K, Register D F and Trajmar S 1983 *Proc. 13th Int. Conf. on Physics of Electronic and Atomic Collisions, Berlin* ed J Eichler *et al* (Amsterdam: North-Holland) Abstracts p 93 and private communication
Ramsauer C 1921 *Ann. Phys., Lpz* **64** 513
Toburen C H, Nakai M Y and Langley R A 1968 *Phys. Rev.* A **171** 114
Wagenaar R W 1984 *PhD Thesis* University of Amsterdam, to be published
Wagenaar R W and de Heer F J 1980 *J. Phys. B: At. Mol. Phys.* **13** 3855
van Wingerden B, Wagenaar R W and de Heer F J 1980 *J. Phys. B: At. Mol. Phys.* **13** 3841